[Frontiers in Bioscience, Landmark, 25, 283-298, Jan 1, 2020]

Simvastatin improves lysosome function via enhancing lysosome biogenesis in endothelial cells

Youzhi Zhang[1,2], Yun-Ting Wang[2], Saisudha Koka[2], Yang Zhang[2], Tahir Hussain[2], Xiang Li[2]

[1]School of Pharmacy, Hubei University of Science and Technology, Xianning, China, [2]Department of Pharmacological and Pharmaceutical Sciences, College of Pharmacy, University of Houston, Houston, TX 77204

TABLE OF CONTENTS

1. ABSTRACT

Nlrp3 inflammasomes were shown to play a critical role in triggering obesity-associated early onsets of cardiovascular complications such as endothelial barrier dysfunction with endothelial hyperpermeability. Statins prevent endothelial dysfunction and decrease cardiovascular risk in patients with obesity and diabetes. However, it remains unclear whether statin treatment for obesity-induced endothelial barrier dysfunction is in part due to the blockade of Nlrp3 inflammasome signaling axis. The results showed that simvastatin, a clinically and widely used statin, prevented free fatty acid-

induced endothelial hyperpermeability and disruption of ZO-1 and VE-cadherin junctions in mouse microvascular endothelial cells (MVECs). This protective effect of simvastatin was largely due to improved lysosome function that attenuated lysosome injury-mediated Nlrp3 inflammasome activation and subsequent release of high mobility group box protein-1 (HMGB1). Mechanistically, simvastatin induces autophagy that promotes removal of damaged lysosomes and also promotes lysosome regeneration that preserves lysosome function. Collectively, simvastatin treatment improves lysosome function via enhancing lysosome biogenesis and its autophagic turnover, which may be an important mechanism to suppress Nlrp3 inflammasome activation and prevents endothelial hyperpermeability in obesity.

2. INTRODUCTION

Endothelial dysfunction is an early onset of vascular diseases in patients with diabetes and obesity (1). Endothelial cells are connected to each other by a complex set of junctional proteins including tight junction ZO-1/2 and occludin and adherens junction protein such as VE-cadherin (2). Down-regulation of inter-endothelial junction proteins is an early event in the development of endothelial barrier dysfunction, which can lead to many pathological consequences including endothelial cell injury, increased leakage of plasma proteins to the interstitial compartment, and enhanced leucocyte transmigration in the vasculature (3, 4).

Statins are pharmacological inhibitors of HMG-CoA reductase that block mevalonate and isoprenoid synthesis and are widely used to treat dyslipidemia (5-7). Due to their pleiotropic effects, the clinical benefits associated with the use of statins to reduce cardiac death and vascular disorders are likely due, in part, to other non-lipid-lowering properties, including anti-inflammation, promoting nitric oxide bioavailability, reducing endothelial barrier dysfunction, and stabilizing atherosclerotic plaques (5, 6, 8, 9). Palmitate is one of the most abundant saturated free fatty acid in the plasma and considered as a typical danger signal associated with vascular diseases in patients with obesity and diabetes (10). We recently demonstrated that palmitate causes lysosome destabilization and activates NOD-like receptor family pyrin domain containing 3 (Nlrp3) inflammasome complex in endothelial cells (10). This inflammasome instigation could be a triggering mechanism elicited by free fatty acids that contributes to the development of endothelial barrier dysfunction and vasculopathy in obesity (10, 11). However, it remains unknown if statins inhibit the barrier dysfunction in obesity and its underlying mechanisms.

In the present study, we tested if statins inhibit endothelial hyperpermeability by free fatty acids via targeting Nlrp3 inflammasomes. We treated endothelial cells with simvastatin, a clinically widely used statin, and observed its effects on palmitate-induced changes in endothelial cell monolayer permeability, junction protein expression, and Nlrp3 inflammasome activation. Our results indicate that, at therapeutically relevant concentrations, simvastatin inhibits palmitate-induced Nlrp3 inflammasome activation, inter-endothelial junction disruption, and barrier dysfunction in endothelial cells. We further demonstrate that simvastatin treatment preserves lysosome function, which may contribute to its inhibitory effects on Nlrp3 inflammasomes in endothelial cells. Our studies thus reveal a potential novel mechanism for the beneficial action of statins on endothelial barrier dysfunction in obesity.

3. MATERIALS AND METHODS

3.1. Cell culture and palmitate

The mouse microvascular endothelial cell (MVEC) line EOMA was purchased from ATCC and cultured as we recently described (12, 13). MVECs were cultured in Dulbecco's modified Eagle's medium (DMEM) (Gibco, USA), containing 10% of fetal bovine serum (Gibco, USA) and 1% penicillin–streptomycin (Gibco, USA). The cells were cultured in a humidified incubator at mixture at 37 °C with 5% CO2 and 95% air. Cells were passaged by trypsinization (Trypsin/EDTA; Sigma, USA), followed by dilution in DMEM medium containing 10 % fetal bovine serum. Sodium palmitate (Sigma) was prepared as previously described (14).

© 1996-2020

3.2. Measurement of endothelial barrier function

The barrier function of the endothelial monolayer was assessed by determining the transendothelial electrical resistance **(**TEER) at low frequency (4000 Hz). Briefly, MVEC were grown on gold electrodes (in 8W10+E arrays) till confluence and maintained in medium with 1% FBS. Cells were challenged with palmitate (50 µM) with or without simvastatin (1-10 µM). TEER was measured using electrical cell-substrate impedance sensing (ECIS) ZΘ system (Applied Biophysics). The changes of TEER for duration of 12 hours were determined. The barrier function was also confirmed by FITC-dextran transwell assay as described previously (10). MVECs were cultured in 24-well transwell plates till confluence and maintained in medium with 1% FBS and treated as indicated for 12 hr. The fluorescent intensity in each well was determined at excitation/emission of 485/530 nm using a fluorescent microplate reader (BMG Labtech).

3.3. Cell viability assay

The cell viability was assessed by lactate dehydrogenase (LDH) assay. LDH activity in the cell culture medium was determined by PierceP^{tm}P LDH Assay Kit (Thermo, IL, USA) according to the manufacture's protocol. The absorbance was spectrophotometrically quantified at 490 nm using CLARIOstar microplate reader (BMG Labtech, Germany). The maximum LDH activity ($LDHR_{max}R$) was obtained from samples treated with lysis buffer. The basal level of LDH activity ($LDHR_0R$) due to spontaneous LDH release was obtained from control samples. The survival was calculated as percentage of ($LDHR_{max}R$-$LDHR_{sample}R$) over ($LDHR_{max}R$-$LDHR_0R$).

3.4. Immunofluorescence microscopic analysis

Cells were grown on eight-well chamber slides till confluence and then treated as indicated and fixed in 4% paraformaldehyde for 15 minutes. Cells were washed in phosphate-buffer saline (PBS), permeabilized in 0.3% Triton X-100/PBS for 15 min, and then incubated for 2 hours at 4°C with incubated with rabbit, rat, or mouse anti-ZO-1 (1:100; Invitrogen), VE-cadherin (1:100; Abcam), anti-TFEB (1:100; Mybiosource). Immunofluorescent staining was performed by incubating slides with Alexa Fluor 488 or Alexa Fluor 555-labeled secondary antibody (1:100, Invitrogen) for 1 hour at room temperature. The samples were fixed, mounted, and visualized using an inverted microscope (Olympus IX73 Fluoview DP-80, Japan).

3.5. Western blot analysis

Cells were lysed using sucrose buffer (20 mM HEPES, 1mM EDTA, 255 mM sucrose, cocktail o protease inhibitors (Roche), pH 7.4) and then whole cell lysates were obtained by centrifugation at 1,000 *g* for 5 min. The cytosolic fractions were prepared by centrifugation of whole cell lysates at 17,000 *g* for 30 min. After boiling for 5 min at 95 °C in a 2× loading buffer, 30 µg of total proteins were separated by a 10% or 15% sodium dodecyl sulfate-polyacrylamide gel electrophoresis (SDS-PAGE). The proteins of these samples were then electrophoretically transferred at 100 V for 1 hour onto a PVDF membrane (Bio-Rad, USA). The membrane was blocked with 5% nonfat milk in Tris-buffered saline-Tween 20. After washing, the membrane was probed with 1:1000 dilution of primary mouse, rat, or rabbit antibodies against anti-ZO-1, VE-cadherin, HMGB1 (Abcam), or following antibodies from Cell signaling including cathepsin B, LC3I/II, Beclin-1, phospho-p70S6 kinase, p70S6 kinase, GAPDH, β-tubulin or β-actin overnight at 4 °C followed by incubation with IRDye fluorescent dyes (IRDye 680RD and IRDye 800CW, 1:15000). The immuno-reactive bands were detected by Licor Odyssey Fc (Licor, USA) instrument methods visualized on the Odyssey Fc Imager. Densitometric analysis of the images was performed using the Image StudioP^{TM}P Software (Licor, USA) as we described previously (15, 16).

3.6. FLICA™ analysis of caspase-1 activation

FLICA™ (Fluorescent Labeled Inhibitor of Caspases) probes were used to detect active caspase-1 enzyme as described (12). Cells were incubated with FLICA reagent (1:100 dilutions in PBS) from a FLICA™ Assay Kit (ImmunoChemistry

© 1996-2020

Table 1. Primers for Real-time PCR

Gene	Forward	Reverse
TFEB	5'-CAGCAGGTGGTGAAGCAAGAGT-3'	5'-TCCAGGTGATGGAACGGAGACT-3'
LC3	5'- CGTCCTGGACAAGACCAAGT-3'	5'-ATTGCTGTCCCGAATGTCTC-3'
LAMP2a	5'-AATCTAAGGAGTTGCCGTTATAC-3'	5'- CCAGTGTCTTCAATCTTGCC-3'
β-actin	5'-TCGCTGCGCTGGTCGTC-3'	5'-GGCCTCGTCACCCACATAGGA-3'

Technologies, LLC, Bloomington, MN) for 1.5 hours at room temperature and then washes three times in PBS. The green fluorescent signal from FLICA™ probes were analyzed with a fluorescence plate reader and used to represent the relative enzyme activity of caspase-1 in cells.

3.7. Lysotracker DND-99 staining of lysosomes

MVECs cultured in eight-well chambered coverslips were treated as indicated and then incubated with 1 μM Lysotracker DND-99 (Invitrogen) in culture medium for 10 min at 37 °C. Cells were washed with fresh medium for three times and analyzed using an inverted microscope (Olympus IX73 Fluoview DP-80, Japan).

3.8. Tandem RFP-GFP-LC3B assay

To analyze the autophagic flux, MVECs were transfected with Premo™ Autophagy Tandem Sensor RFP-GFP-LC3B (Thermo Fisher Scientific) as described previously (17, 18). After 48 h, cells were treated with 10 μM simvastatin, 10 μM chloroquine (Sigma), or 200 μM Leupeptin A (Sigma) for 18 h. Cells were fixed in freshly prepared 4% PFA, washed in PBS, and then mounted. Autophagic flux was determined by evaluating patterns of GFP and RFP dots using an inverted microscope (Olympus IX73 Fluoview DP-80, Japan).

3.9. Acridine orange staining of lysosomes

MVECs cultured in eight-well chamber slides were treated as indicated and then incubated with 2 μg/mL acridine orange (Cayman chemical) for 17 min at 37 °C, rinsed with PBS. Cells in chamber slides were immediately analyzed and photographed. Gly-Phe-β-naphthylamide (GPN, Cayman chemical), a lysosome-disrupting agent, was used as a positive control for increased lysosome permeability. Then the intensity ratio of red-to-green fluorescence of cells was obtained by an Acoustic Focusing Cytometer (Attune NxT, ThermoFisher Scientific, USA).

3.10. RNA interference

Small interference RNAs (siRNAs) for TFEB gene (siTFEB) and scramble control siRNA were commercially available (Santa Cruz Biotechnology, CA). Transfection of siRNA was performed using the siLentFect Lipid Reagent (Bio-Rad, CA, USA) according to the manufacturer's instructions.

3.11. Real-time reverse transcription polymerase chain reaction (RT-PCR)

Total RNA from cells was extracted with Aurum Total RNA isolation kit (Bio-Rad) according to the manufacturer's protocol. One-microgram aliquots of total RNA from each sample were reverse-transcribed into cDNA by using a first-strand cDNA synthesis kit (Bio-Rad). Equal amounts of the reverse transcriptional products were subjected to PCR amplification PrimePCR™ SYBR® Green Assay on a CFX Connect Real-Time PCR Detection System (Bio-Rad). The sequences of primers for target genes are listed in Table 1.

3.12. Statistics analysis

Data are presented as means ± standard deviation. Significant differences between and within multiple groups were examined using one-way ANOVA test followed by Bonfferroni's multiple-range test. A Students *t*-test was used to detect significant difference between two groups. The statistical

© 1996-2020

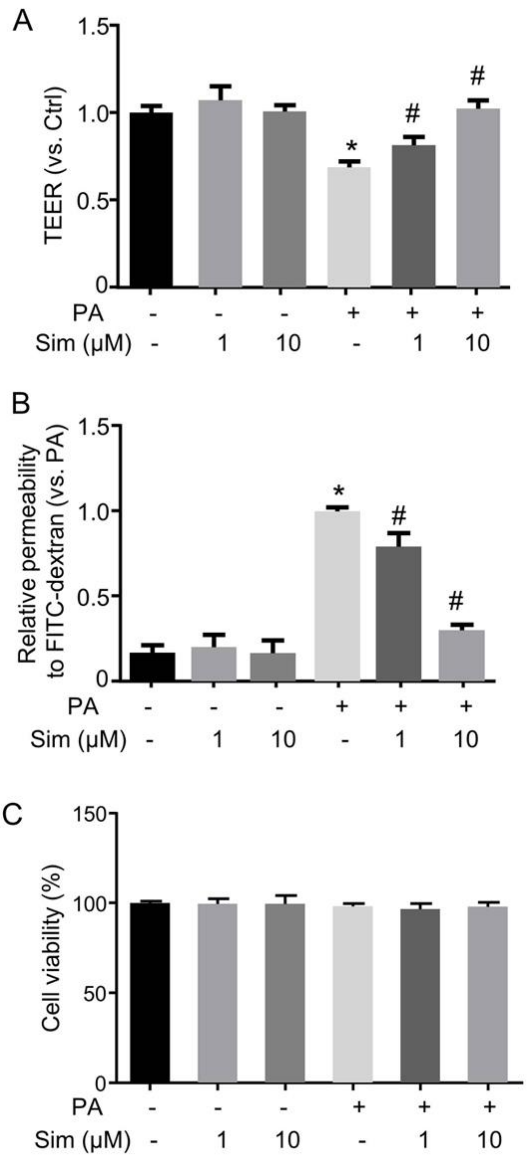

Figure 1. Simvastatin protects palmitate-induced endothelial hyperpermeability. MVECs were treated with palmitate (PA, 50 μM) in the presence of vehicle (PBS) or simvastatin (Sim, 1-10 μM) for 12 hours. (A) EC permeability was measured by transendothelial electrical resistance (TEER). (n=4). (B) EC permeability was determined by measuring the amount of FITC-dextran that crossed the endothelial monolayer cultured on the inserts of transwell (n=4). (C) Cell viability by LDH assay (n=4). *P<0.05 vs. untreated control; #P<0.05 vs. PA alone

analysis was performed by GraphPad Prism 6.0 software. *P*<0.05 was considered statistically significant.

4. RESULTS

4.1. Simvastatin alleviates palmitate-induced endothelial hyperpermeability

To examine the effects of simvastatin on endothelial hyperpermeability, we first used ECIS technology to measure the changes of TEER in response to 50 μM palmitate for 12 hours in presence or absence of simvastatin. As shown in Figure 1A, palmitate reduced the TEER of the MVEC monolayer and simvastatin significantly inhibited this response at 10 μM. In contrast, simvastatin at 1 μM has only negligible effect. FITC-dextran transwell assay was then used to confirm the cell permeability to high-molecular-weight molecules. As shown in Figure 1B, we observed significantly increased FITC-dextran molecules across the MVEC monolayer indicating the increased permeability of endothelial cell monolayers by palmitate, and simvastatin reduced this effect. The changes in the endothelial permeability by 50 μM palmitate were not associated with increased cell death because no changes in cell viability were observed (Figure 1C). Together, these results suggest that simvastatin exerts protective effects on palmitate-induced endothelial hyperpermeability.

4.2. Simvastatin counteracts palmitate-induced down-regulation of inter-endothelial junction proteins

Endothelial hyperpermeability is associated with down-regulation of junction protein ZO-1 and VE-cadherin (10, 11). By immunofluorescence studies, we found that simvastatin dramatically reversed palmitate-induced downregulation of tight junction protein ZO-1 and adherens junction protein VE-cadherin (Figure 2A). This inhibitory effect of simvastatin on ZO1 and VE-cadherin was confirmed by Western blot analysis (Figure 2B).

4.3. Simvastatin inhibits palmitate-induced lysosome injury and Nlrp3 inflammasome activity

Our recent study demonstrated that palmitate-induced endothelial hyperpermeability

© 1996-2020

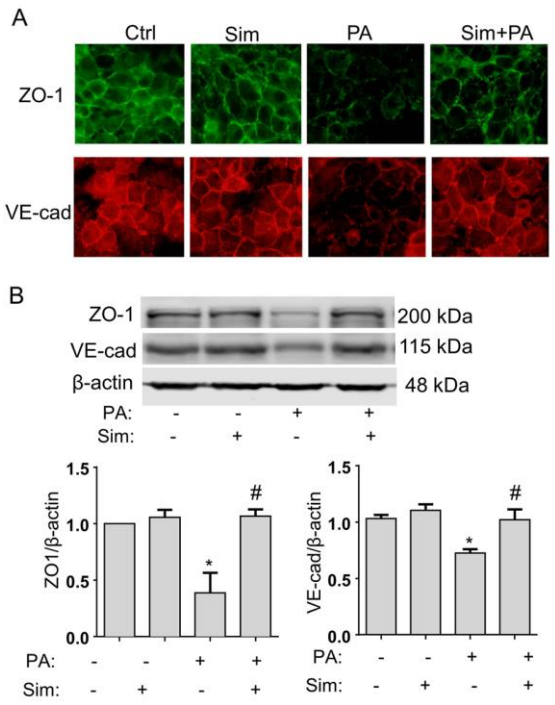

Figure 2. Simvastatin blunts palmitate-induced tight-junction dysfunction. MVECs were treated with palmitate (PA, 50 μM) in the presence of vehicle (PBS) or simvastatin (Sim, 10 μM) for 12 hours. (A) Representative fluorescence images show the cell membrane fluorescence of ZO-1 (Alexa Fluor 488) and or VE-cadherin (Alexa Fluor 555) from at least three independent experiments. (B) Representative immunoblot (top) and band intensity quantification (bottom) for ZO-1 and VE-cadherin expression in response to palmitate with or without simvastatin (n=4). β-actin was an internal loading control. *P<0.05 vs. untreated control; #P<0.05 vs. PA alone.

was associated with increased Nlrp3 inflammasome activation (10), which caused increased release of HMGB1, a novel endothelial permeability factor (12, 19). The inflammasome activity induced by palmitate was attributed to events including lysosome destabilization and consequent lysosomal release of cathepsin B but not to reactive oxygen species (ROS) (10). In the present study, we examined whether or not simvastatin prevents palmitate-induced lysosome injury and Nlrp3 inflammasome activity. Lysotracker DND-99 is a lysosomotropic dye that stains lysosomes with acidic pH, and decreases in lysotracker DND-99 intensity suggest disruptions in lysosomal function, integrity, or quantity (20). As shown in Figure 3A, palmitate significantly decreases the lysotracker staining, which was preserved by simvastatin. We also found that simvastatin abolished the cytosolic expression of cathepsin B upon palmitate stimulation (Figure 3B), suggesting that simvastatin prevents lysosomal release of cathepsin B. Thus, these data indicate that simvastatin preserves lysosome integrity and prevents cathepsin B release. We then evaluated Nlrp3 inflammasome activity by measuring two marker events including the caspase-1 activity assay and IL-18 production. It was found that simvastatin markedly suppressed the palmitate-induced activation caspase-1 (Figure 3C) and the release of and IL-18 (Figure 3D). These data confirm that caspase-1 is activated by palmitate, which is blocked by simvastatin. As shown in Figure 3E, simvastatin also dramatically inhibited palmitate-induced release of HMGB1 protein into the culture media. As a comparison, no significant effects were observed in the HMGB1 level in whole cell lysates.

4.4. Simvastatin increases autophagy signaling and lysosome biogenesis

Simvastatin dose-dependently increased the protein expression of LC3-II, an autophagy marker (Figure 4A). Simvastatin can also increase LC3-II when autophagy flux was blocked by chloroquine (Figure 4A). We noticed that simvastatin did not affect Beclin1, a modulator for autophagosome assembly. These data suggest that simvastatin might increase autophagosome biogenesis but not enhance its assembly.

We next monitored the autophagic flux by expressing tandem RFP-GFP–LC3 genes. The tandem RFP-GFP-LC3B protein includes an acid-insensitive RFP and an acid-sensitive GFP. The expression pattern of GFP-RFP-LC3 constructs is dependent on the fusion of autophagosomes with lysosomes, lysosomal acidification and degradation capacity (21). As shown in Figure 4B, simvastatin elevated the number of yellow/orange puncta (autophagosomes are $RFPP^{+}PGFPP^{+}P$) and the red puncta (autophagolysosomes are $RFPP^{+}PGFPP^{-}P$) in the merged image compared to control. We further determined the tandem RFP-GFP-LC3 expression pattern in merged images by two autophagic flux inhibitors. First, chloroquine neutralizes lysosomal pH and inhibits lysosome

© 1996-2020

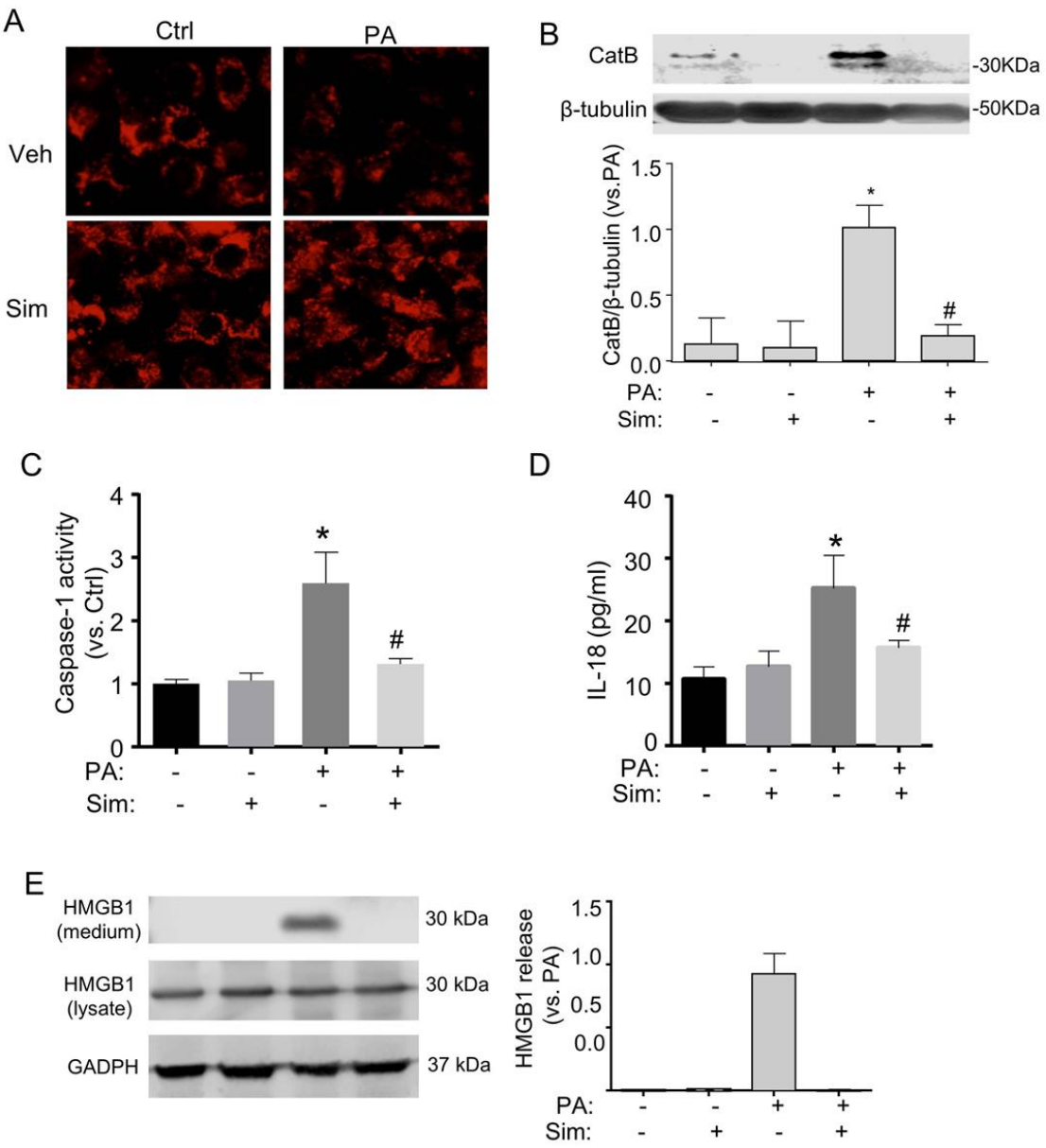

Figure 3. Simvastatin inhibits palmitate-induced lysosome injuries and Nlrp3 inflammasome activity. MVECs were treated with palmitate (PA, 50 μM) in the presence of vehicle (PBS) or simvastatin (Sim, 10 μM) for indicated hours. (A) Representative fluorescence images show the lysotracker DND-99 staining in acidic lysosomes (PA 12 hours) from three independent experiments. (B) Western blot analysis of cathepsin B (CatB) expression in cytosolic fractions (PA 12 hours) (n=4). β-tubulin is a loading control. (C) Summarized data show the caspase-1 activation (PA 12 hours) by FLICA assay (n=4). (D) Summarized data showing IL-18 production (PA 48 hours) by ELISA (n=4). (E) Western blot documents and summarized data showing the expression of HMGB1 in either cell culture medium or cell lysate (PA 12 hours) (n = 4). *P<0.05 vs. untreated control; #P<0.05 vs. PA alone

fusion with autophagosome, and thereby results in increased autophagosome accumulation and but decreased formation of autophagolysosomes. Consistently, chloroquine increased the number of yellow/orange punta and red puncta were barely observed, suggesting that it abolished the formation of autophagolysosomes and thus accumulated autophagosomes. Leupeptin is an

© 1996-2020

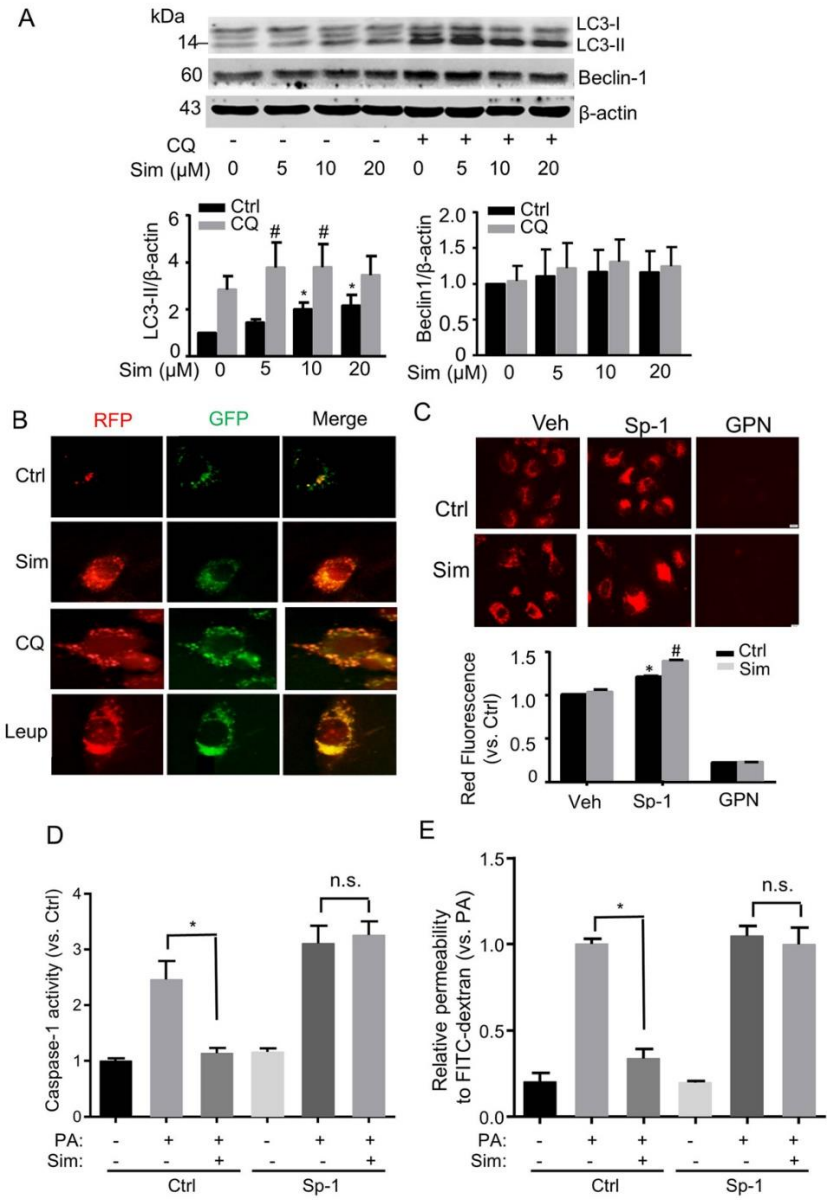

Figure 4. Simvastatin induces autophagy and lysosome biogenesis. (A) MVECs were treated with simvastatin (Sim, 0, 5, 10 and 20 μM) with or without chloroquine (CQ, 10 μM) for 18 h. Representative Western blots show the expression of autophagosome marker proteins LC3II, Beclin-1, or β-actin. Summarized data show the relative expression of LC3II or Beclin-1 compared to β-actin (n=4). *P<0.05 vs. untreated control; #P<0.05 Sim+CQ *vs.* Sim alone. (B) MVECs were transfected with tandem RFP-GFP-LC3B and then treated with PBS control (Ctrl), simvastatin (10 μM), chloroquine (10 μM), or leupeptin A (Leup, 200 μM) for 18 h. Representative fluorescence images show the autophagosomes and autophagolysosomes from at least three independent experiments. Autophagosomes were visualized as yellow or orange puncta (RFP-GFP-LC3) in merged images, whereas red puncta (RFP-LC3) in merged images represent autophagolysosomes since acidification abolishes green fluorescence. Sample without either simvastatin or chloroquine was considered as vehicle control. (C) MVECs were treated without or with simvastatin (Sim, 10 μM) in the absence or presence of autophagosome inhibitor Spautin-1 (Sp-1, 10 μM) for 18 h. MVECs were also treated without or with simvastatin for 16 h and then GPN (200 μM) was added and incubated for additional 4 h. Representative fluorescence images show the acridine orange staining in acidic organelles (lysosomes and autophagolysosomes). Summarized data show the red fluorescence intensity of acridine orange staining by flow cytometer analysis (n=6). *P<0.05 vs. Veh Ctrl; #P<0.05 vs. Sp-1 alone. (D) and (E) Summarized data show the effects of simvastatin (Sim, 10 μM) and/or Spautin-1 (Sp-1, 10 μM) on palmitate (PA, 50 μM for 12 hours)-induced caspase-1 activation by FLICA assay or EC permeability by FITC-dextran assay (n=4). *P<0.05; n.s. (not significant)

© 1996-2020

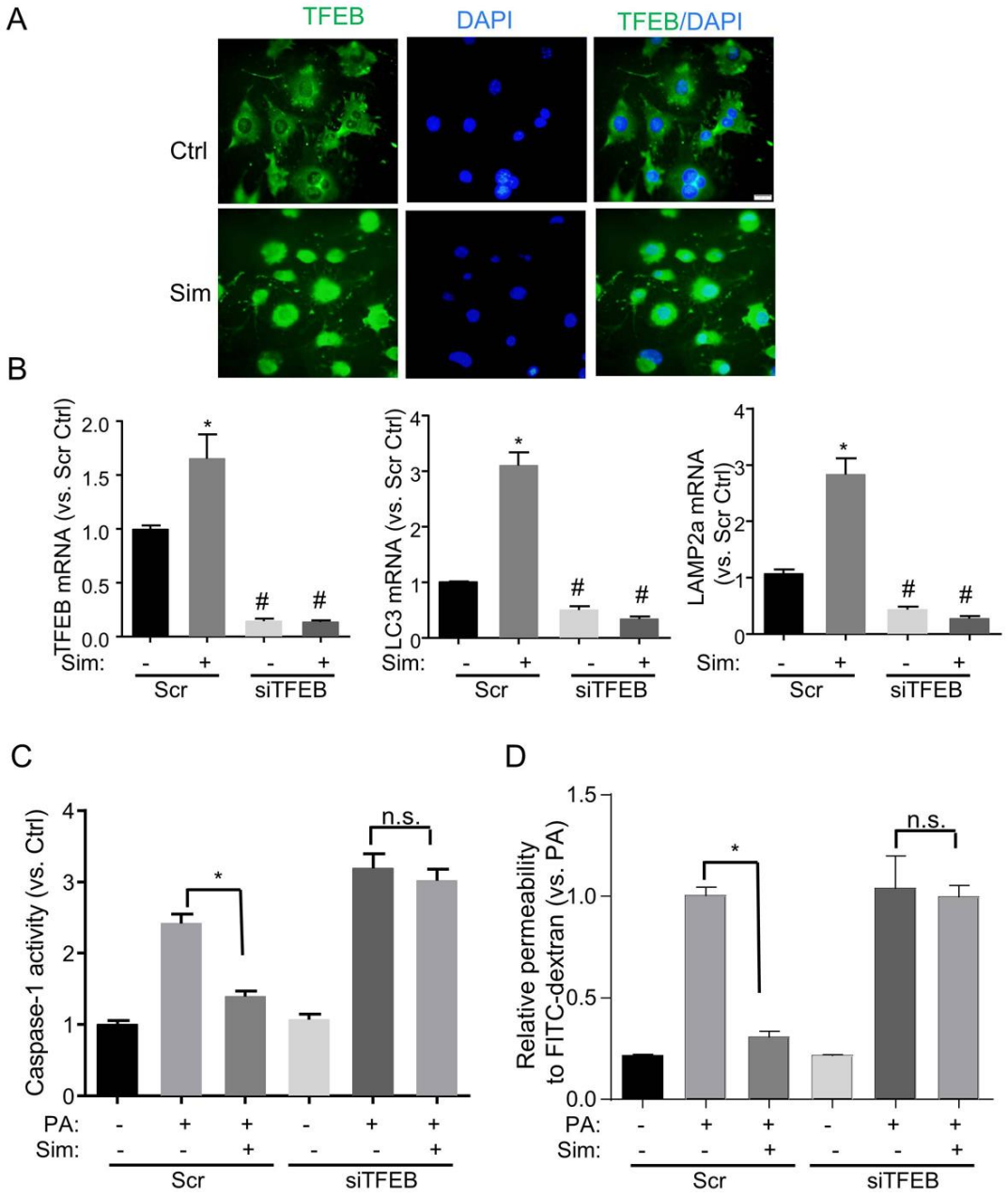

Figure 5. Simvastatin induces activation of TFEB in MVECs. (A) Representative immunofluorescence images of TFEB show the nuclear translocation of TFEB by simvastatin (Sim, 10 μM for 2 h) from four independent experiments. (B) Real-time PCR quantification shows the effects of simvastatin (10 μM for 2 h) on mRNA levels of TFEB, LC3, and LAMP2a in MVECs that were transfected with scramble (Scr) or TFEB siRNA (siTFEB) for 24 h (n=4). *P<0.05 vs. Scr Ctrl; #P<0.05 vs. Scr+Sim. (C) and (D) Summarized data show the effects of simvastatin (10 μM) on PA (50 μM, 12 hours)-induced caspase-1 activation by FLICA assay or EC permeability by FITC-dextran assay in MVECs that were transfected with scramble (Scr) or TFEB siRNA (siTFEB) for 24 h (n=4). *P<0.05; n.s. (not significant).

autophagic flux inhibitor that blocks lysosome protease activity and thereby inhibits autophagolysosome degradation without affecting lysosomal pH. As expected, leupeptin increased the number of the red puncta (autophagolysosome) as well as the

© 1996-2020

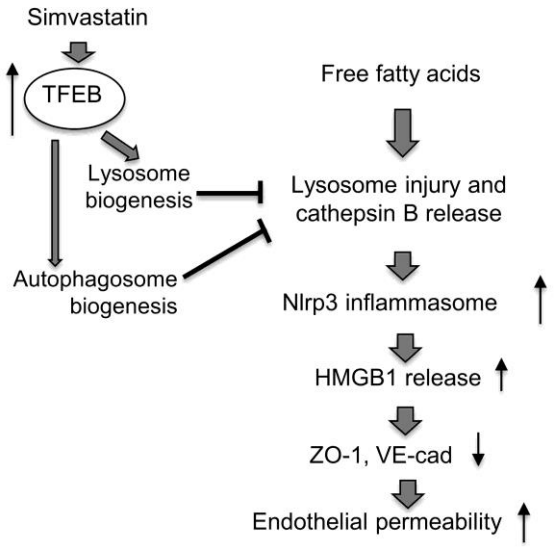

Figure 6. Proposed model for the protective role of simvastatin in free fatty acid-induced endothelial hyperpermeability.

yellow/orange puncta (autophagolysosome) reflecting a defective autophagolysosomal degradation pathway. We noticed that simvastatin-treated cells showed more numbers of red puncta than leupeptin (Figure 4B), suggesting that simvastatin also increases lysosome biogenesis.

Considering lysosome itself as a cargo for autophagy pathway, we examined whether or not inhibition of autophagy induction could result in lysosome accumulation. Acridine orange stains acidic organelles including lysosomes and autophagolysosomes. We found that spauntin-1, an autophagy inhibitor, significantly increased acridine orange intensity, suggesting that spautin-1 blocked autophagy-dependent lysosome degradation at basal condition (Figure 4C). Simvastatin further enhanced acridine orange intensity when autophagy is inhibited, suggesting that simvastatin increased lysosome biogenesis. However, simvastatin alone had no significant effect. These data suggest simvastatin induces autophagy signaling that promotes lysosome degradation; meanwhile, simvastatin increases lysosome biogenesis. We further found that the inhibitory effects of simvastatin on palmitate-induced Nlrp3 inflammasome activity (Figure 4D) and permeability (Figure 4E) were reversed when autophagy is inhibited by spautin-1.

4.5. Simvastatin induced TFEB activation

Transcriptional factor EB (TFEB) is a master regulator involved in autophagy signaling and lysosomal biogenesis (22, 23). As shown in Figure 5A, simvastatin markedly increased TFEB expression in the nuclei implicating that simvastatin induces nuclear translocation of TFEB and consequent transcription of genes involved in autophagy and lysosome biogenesis. We also demonstrated that simvastatin induced up-regulation of genes involved in TFEB-autophagy-lysosome signaling including TFEB, LC3, and LAMP2a, which was blocked by TFEB gene silencing (Figure 5B). Inhibition of mTOR has been shown to enhance TFEB activity (15, 24, 25). The mTOR activity is determined by the phosphorylation of S6K. However, simvastatin had no effects on S6K phosphorylation (data not shown). It is suggested that simvastatin may activate TFEB pathway in mTOR-independent manner. Consistently, TFEB gene silencing also prevented the inhibitory effects of simvastatin on palmitate-induced Nlrp3 inflammasome activity (Figure 5C) and permeability (Figure 5D).

5. DISCUSSION

The aim of the present study is to explore the effects and underlying mechanisms of statins on endothelial hyperpermeability induced by free fatty acid palmitate. Our study demonstrated that simvastatin effectively reversed Nlrp3 inflammasome activation, junction disruption, and endothelial hyperpermeability by palmitate. Further, we uncovered a previously undefined lysosome protective role of simvastatin in suppressing Nlrp3 inflammasomes, which may contribute to its pleiotropic effects to reduce cardiovascular risk.

Clinical trials indicate that statins reduce cardiovascular disorders and improve vascular function in patients with diabetes and obesity (26). However, no clinical study has demonstrated whether statins benefit patients with improved endothelial barrier function, especially before the development of more advanced vasculopathy such as atherosclerosis. In this study, the protective effects of simvastatin on the barrier function were first demonstrated by ECIS. At low frequency of 4000 Hz,

© 1996-2020

ECIS detects mainly paracellular impedance, which inversely correlates with the integrity of inter-endothelial junctions. Our data indicate that simvastatin remarkably inhibited palmitate-induced decreases in TEER. In addition, by measuring the amount of FITC-dextran molecules across the endothelial monolayers, we confirmed that simvastatin restored the barrier function of endothelial monolayer to high-molecular-weight molecules. Our data further demonstrated that simvastatin effectively prevent palmitate-induced disruption of ZO-1 and VE-cadherin junctions. These findings are consistent with the inhibitory effect of statins on endothelial permeability or junction protein expressions in other pathological conditions such as diabetes and high glucose (19, 27, 28). A recent study showed a basal level of transcytosis of palmitate via endothelial cell monolayers and TNF enhanced such transcytosis of palmitate (29). It is possible that palmitate causes primarily junction disruption but, in the meantime, increases transcytosis machinery. Our current findings provide first evidence that statins can be used to treat obesity associated endothelial barrier dysfunction, which may be in part due to recovery of inter-endothelial junction integrity.

Recent studies unravel a critical role of Nlrp3 inflammasome in the development of endothelial dysfunction in obesity and diabetes (10, 11, 30). Assembly of Nlrp3 inflammasome complex causes the caspase-1 activation and subsequent secretion of nuclear protein HMGB1, which causes endothelial barrier dysfunction in obesity and diabetes (10, 19, 30). In the present study, our data for the first time showed that simvastatin inhibited Nlrp3 inflammasome activation and HMGB1 release stimulated by free fatty acid. Our novel findings suggest that the pleiotropic property of statins to reduce cardiovascular risk in obesity may be attributed to inhibition of Nlrp3 inflammasomes and reduction of HMGB1 secretion.

Our previous studies demonstrated that the lysosome destabilization and consequent cathepsin B release mediates the Nlrp3 inflammasome activation by free fatty acids or in high fat diet-induced obesity (10). Here, we demonstrated that prevention of lysosome-cathepsin B mediates the protective effect of simvastatin on Nlrp3 inflammasome activation by free fatty acid, indicating a novel action of simvastatin on lysosomes. Our finding is in consistent with the finding that lysosome stabilization agents attenuate Nlrp3 inflammasome activation in mouse model of coronary arteritis (12). Loss of lysosome functions causes many injurious effects such as impaired mitochondrial respiration, oxidative stress, or apoptosis. Therefore, our findings support the view that preservation of lysosome function by simvastatin represents one key pleiotropic effect on cardiovascular system that may not only inhibit inflammasome signaling but also prevent other lysosome injury associated detrimental effects.

Another important finding of the present study is that simvastatin-mediated lysosome protection is through autophagy-lysosome signaling pathway. Autophagy is a highly conserved catabolic process and degrades unhealthy organelles and long-lived proteins by lysosome machinery (31-34). Simvastatin or atorvastatin induced autophagy via non-lipid lower effects in vascular cells such as in coronary or aortic smooth muscle cells (35, 36) and in liver sinusoidal endothelial cells (37). Consistently, our data demonstrated an inducing role of simvastatin in autophagosome formation and its flux in MVECs as evidenced by (1) enhanced LC3 expression even when autophagic flux was blocked; (2) increased formation of autophagolysosomes. Spautin-1 is a specific inhibitor of autophagy that targets its assembly machinery. We found that spautin-1 accumulated lysosomes indicating that the autophagy promotes lysosome degradation. More interestingly, our data demonstrated that simvastatin enhanced lysosome accumulation when autophagosome formation was inhibited by spautin-1, indicating that lysosome biogenesis was initiated by simvastatin. Interestingly, spautin-1 reverses the protective effects of simvastatin on palmitate-induced Nlrp3 inflammasome activity and endothelial permeability. Together, these findings support the view that simvastatin preserves lysosome function by enhancing autophagy-mediated lysosome degradation as well as inducing lysosome biogenesis to replace injured lysosomes. It should be noted that the Nlrp3 inflammasome complex itself could be a substrate of autophagy pathway (38). Therefore, it is also possible that simvastatin may suppress Nlrp3

© 1996-2020

inflammasome activity via autophagy-mediated degradation of inflammasome components. Future studies are needed to decipher the precise roles of autophagy in mediating the protective effects of simvastatin on Nlrp3 inflammasome activation. Nonetheless, in the early stage of cardiovascular complications in obesity, simvastatin may exert its lysosome protective effect by eliminating mildly injured lysosomes in autophagy-dependent manner and replacing them with nascent functional lysosomes.

Lastly, our data suggest that TFEB may serve as a molecular mediator for simvastatin-induced autophagy-lysosome signaling. Recent studies highlight TFEB as a master controller of genes involved in autophagy signaling and lysosome biogenesis (39-44). The role of TFEB in regulation of cardiovascular functions has only recently become clearer. In particular, activation of TFEB by trehalose ameliorates atherosclerosis development in mice by promoting lysosome regeneration, autophagy induction, and inhibition of inflammasome activity in macrophages (45). Endothelial specific overexpression of TFEB suppresses endothelial inflammation and attenuate atherosclerosis in mice (46). The present study, for the first time, demonstrated that simvastatin induces autophagy and lysosome signaling via TFEB activation in MVECs. More importantly, TFEB-mediated autophagy and lysosome signaling was shown to mediate the protective effects of simvastatin on palmitate-induced Nlrp3 inflammasome activation and endothelial permeability. Inhibition of mTOR was shown to enhance TFEB activity (15, 24, 25). Our previous studies demonstrated that simvastatin inhibits Rac1-dependent mTOR activation via non-lipid lowering effects in vascular smooth muscle cells (36). Intriguingly, our unpublished data found that simvastatin did not affect mTOR activity indicating an mTOR-independent activation of TFEB in MVECs. Future studies will explore the precise mechanism of TFEB activation by simvastatin. Moreover, the *in vivo* role of simvastatin-TFEB-autophagy-lysosome axis in protecting endothelial dysfunction in animal models of obesity will be investigated.

In summary, our findings support the model (Figure 6) that simvastatin improves lysosome function through TFEB-dependent autophagy-lysosome signaling, which leads to inhibition of Nlrp3 inflammasome and HMGB1 release in MVECs. This lysosome protective effect of simvastatin contributes to the recovery of junction integrity and endothelial permeability. These findings provide novel insights into understanding the pleiotropic effects of statins on reducing cardiovascular complications in obesity.

6. ACKNOWLEDGMENT

The authors have no conflict of interest. This study was supported by the faculty development funds of College of Pharmacy at University of Houston, the grants from the National Institutes of Health (HL122769 and HL122937), and National Natural Science Foundation of China (NO.81603110).

7. REFERENCES

1. P. A. Stapleton, M. E. James, A. G. Goodwill and J. C. Frisbee: Obesity and vascular dysfunction. Pathophysiology, 15(2), 79-89 (2008) DOI: 10.1016/j.pathophys.2008.04.007

2. E. Dejana, M. Corada and M. G. Lampugnani: Endothelial cell-to-cell junctions. FASEB J, 9(10), 910-8 (1995) DOI: 10.1096/fasebj.9.10.7615160

3. E. Vandenbroucke, D. Mehta, R. Minshall and A. B. Malik: Regulation of endothelial junctional permeability. Ann N Y Acad Sci, 1123, 134-45 (2008) DOI: 10.1196/annals.1420.016

4. S. Hernandez, B. Chavez Munguia and L. Gonzalez-Mariscal: ZO-2 silencing in epithelial cells perturbs the gate and fence function of tight junctions and leads to an atypical monolayer architecture. Exp Cell Res, 313(8), 1533-47 (2007) DOI: 10.1016/j.yexcr.2007.01.026

5. D. Tousoulis, E. Oikonomou, G. Siasos

© 1996-2020

and C. Stefanadis: Statins in heart failure--With preserved and reduced ejection fraction. An update. Pharmacol Ther, 141(1), 79-91 (2014)
DOI: 10.1016/j.pharmthera.2013.09.001

6. D. X. Bu, G. Griffin and A. H. Lichtman: Mechanisms for the anti-inflammatory effects of statins. Curr Opin Lipidol, 22(3), 165-70 (2011)
DOI: 10.1097/MOL.0b013e3283453e41

7. P. Libby, P. M. Ridker, G. K. Hansson and A. Leducq Transatlantic Network on: Inflammation in atherosclerosis: from pathophysiology to practice. J Am Coll Cardiol, 54(23), 2129-38 (2009)
DOI: 10.1016/j.jacc.2009.09.009

8. J. R. Jacobson: Statins in endothelial signaling and activation. Antioxid Redox Signal, 11(4), 811-21 (2009)
DOI: 10.1089/ars.2008.2284

9. R. P. Mason, M. F. Walter and R. F. Jacob: Effects of HMG-CoA reductase inhibitors on endothelial function: role of microdomains and oxidative stress. Circulation, 109(21 Suppl 1), II34-41 (2004)
DOI: 10.1161/01.CIR.0000129503.62747.03

10. L. Wang, Y. Chen, X. Li, Y. Zhang and E. Gulbins: Enhancement of endothelial permeability by free fatty acid through lysosomal cathepsin B-mediated Nlrp3 inflammasome activation. Oncotarget, 7(45), 73229-73241 (2016)
DOI: 10.18632/oncotarget.12302

11. Y. Chen, A. L. Pitzer, X. Li, P. L. Li, L. Wang and Y. Zhang: Instigation of endothelial Nlrp3 inflammasome by adipokine visfatin promotes inter-endothelial junction disruption: role of HMGB1. J Cell Mol Med, 19(12), 2715-27 (2015)
DOI: 10.1111/jcmm.12657

12. Y. Chen, X. Li, K. M. Boini, A. L. Pitzer, E. Gulbins, Y. Zhang and P. L. Li: Endothelial Nlrp3 inflammasome activation associated with lysosomal destabilization during coronary arteritis. Biochim Biophys Acta, 1853(2), 396-408 (2015)
DOI: 10.1016/j.bbamcr.2014.11.012

13. Y. Guan, X. Li, M. Umetani, K. M. Boini, P. L. Li and Y. Zhang: Tricyclic antidepressant amitriptyline inhibits autophagic flux and prevents tube formation in vascular endothelial cells. Basic Clin Pharmacol Toxicol 124, 370-384 (2019)
DOI: 10.1111/bcpt.13146

14. H. Wen, D. Gris, Y. Lei, S. Jha, L. Zhang, M. T. Huang, W. J. Brickey and J. P. Ting: Fatty acid-induced NLRP3-ASC inflammasome activation interferes with insulin signaling. Nat Immunol, 12(5), 408-15 (2011)
DOI: 10.1038/ni.2022

15. C. Zhang, K. M. Boini, M. Xia, J. M. Abais, X. Li, Q. Liu and P. L. Li: Activation of Nod-like receptor protein 3 inflammasomes turns on podocyte injury and glomerular sclerosis in hyperhomocysteinemia. Hypertension, 60(1), 154-62 (2012)
DOI: 10.1161/HYPERTENSIONAHA.111.189688

16. P. Zhang, Y. Guan, J. Chen, X. Li, B. K. McConnell, W. Zhou, K. M. Boini and Y. Zhang: Contribution of p62/SQSTM1 to PDGF-BB-induced myofibroblast-like phenotypic transition in vascular smooth

© 1996-2020

muscle cells lacking Smpd1 gene. Cell Death Dis, 9(12), 1145 (2018)
DOI: 10.1038/s41419-018-1197-2

17. X. Cao, Y. Zhang, Y. Chen, Y. Qiu, M. Yu, X. Xu, X. Liu, B. F. Liu, L. Zhang and G. Zhang: Synthesis and Biological Evaluation of Fused Tricyclic Heterocycle Piperazine (Piperidine) Derivatives As Potential Multireceptor Atypical Antipsychotics. J Med Chem (2018)
DOI: 10.1021/acs.jmedchem.8b01096

18. Y. Zhang, M. Xu, M. Xia, X. Li, K. M. Boini, M. Wang, E. Gulbins, P. H. Ratz and P. L. Li: Defective autophagosome trafficking contributes to impaired autophagic flux in coronary arterial myocytes lacking CD38 gene. Cardiovasc Res, 102(1), 68-78 (2014)
DOI: 10.1093/cvr/cvu011

19. Z. H. Lv, T. A. Phuong, S. J. Jin, X. X. Li and M. Xu: Protection by simvastatin on hyperglycemia-induced endothelial dysfunction through inhibiting NLRP3 inflammasomes. Oncotarget, 8(53), 91291-91305 (2017)
DOI: 10.18632/oncotarget.20443

20. N. Raben, L. Shea, V. Hill and P. Plotz: Monitoring autophagy in lysosomal storage disorders. Methods Enzymol, 453, 417-49 (2009)
DOI: 10.1016/S0076-6879(08)04021-4

21. S. Kimura, T. Noda and T. Yoshimori: Dissection of the autophagosome maturation process by a novel reporter protein, tandem fluorescent-tagged LC3. Autophagy, 3(5), 452-60 (2007)
DOI: 10.4161/auto.4451

22. C. Settembre, C. Di Malta, V. A. Polito, M. Garcia Arencibia, F. Vetrini, S. Erdin, S. U. Erdin, T. Huynh, D. Medina, P. Colella, M. Sardiello, D. C. Rubinsztein and A. Ballabio: TFEB links autophagy to lysosomal biogenesis. Science, 332(6036), 1429-33 (2011)
DOI: 10.1126/science.1204592

23. M. Sardiello, M. Palmieri, A. di Ronza, D. L. Medina, M. Valenza, V. A. Gennarino, C. Di Malta, F. Donaudy, V. Embrione, R. S. Polishchuk, S. Banfi, G. Parenti, E. Cattaneo and A. Ballabio: A gene network regulating lysosomal biogenesis and function. Science, 325(5939), 473-7 (2009)
DOI: 10.1126/science.1174447

24. M. Araki and K. Motojima: Hydrophobic statins induce autophagy in cultured human rhabdomyosarcoma cells. Biochem Biophys Res Commun, 367(2), 462-7 (2008)
DOI: 10.1016/j.bbrc.2007.12.166

25. A. Parikh, C. Childress, K. Deitrick, Q. Lin, D. Rukstalis and W. Yang: Statin-induced autophagy by inhibition of geranylgeranyl biosynthesis in prostate cancer PC3 cells. Prostate, 70(9), 971-81 (2010)
DOI: 10.1002/pros.21131

26. R. Collins, J. Armitage, S. Parish, P. Sleight and R. Peto: Effects of cholesterol-lowering with simvastatin on stroke and other major vascular events in 20536 people with cerebrovascular disease or other high-risk conditions. Lancet, 363(9411), 757-67 (2004)
DOI: 10.1016/S0140-6736(04)15690-0

27. J. Li, J. J. Wang, D. Chen, R. Mott, Q. Yu, J. X. Ma and S. X. Zhang: Systemic administration of HMG-CoA reductase inhibitor protects the blood-retinal barrier and ameliorates retinal inflammation in type 2 diabetes. Exp Eye Res, 89(1), 71-

© 1996-2020

8 (2009)
DOI: 10.1016/j.exer.2009.02.013

28. H. Peng, P. Luo, Y. Li, C. Wang, X. Liu, Z. Ye, C. Li and T. Lou: Simvastatin alleviates hyperpermeability of glomerular endothelial cells in early-stage diabetic nephropathy by inhibition of RhoA/ROCK1. PLoS One, 8(11), e80009 (2013)
DOI: 10.1371/journal.pone.0080009

29. W. Li, X. Yang, T. Zheng, S. Xing, Y. Wu, F. Bian, G. Wu, Y. Li, J. Li, X. Bai, D. Wu, X. Jia, L. Wang, L. Zhu and S. Jin: TNF-alpha stimulates endothelial palmitic acid transcytosis and promotes insulin resistance. Sci Rep, 7, 44659 (2017)
DOI: 10.1038/srep44659

30. Y. Chen, L. Wang, A. L. Pitzer, X. Li, P. L. Li and Y. Zhang: Contribution of redox-dependent activation of endothelial Nlrp3 inflammasomes to hyperglycemia-induced endothelial dysfunction. J Mol Med (Berl), 94(12), 1335-1347 (2016)
DOI: 10.1007/s00109-016-1481-5

31. B. Levine and G. Kroemer: Autophagy in the pathogenesis of disease. Cell, 132(1), 27-42 (2008)
DOI: 10.1016/j.cell.2007.12.018

32. X. Li, M. Xu, A. L. Pitzer, M. Xia, K. M. Boini, P. L. Li and Y. Zhang: Control of autophagy maturation by acid sphingomyelinase in mouse coronary arterial smooth muscle cells: protective role in atherosclerosis. J Mol Med (Berl), 92(5), 473-85 (2014)
DOI: 10.1007/s00109-014-1120-y

33. Y. Kabeya, N. Mizushima, T. Ueno, A. Yamamoto, T. Kirisako, T. Noda, E. Kominami, Y. Ohsumi and T. Yoshimori: LC3, a mammalian homologue of yeast Apg8p, is localized in autophagosome membranes after processing. EMBO J, 19(21), 5720-8 (2000)
DOI: 10.1093/emboj/19.21.5720

34. Z. Xie and D. J. Klionsky: Autophagosome formation: core machinery and adaptations. Nat Cell Biol, 9(10), 1102-9 (2007)
DOI: 10.1038/ncb1007-1102

35. D. Liu, W. Cui, B. Liu, H. Hu, J. Liu, R. Xie, X. Yang, G. Gu, J. Zhang and H. Zheng: Atorvastatin protects vascular smooth muscle cells from TGF-beta1-stimulated calcification by inducing autophagy via suppression of the beta-catenin pathway. Cell Physiol Biochem, 33(1), 129-41 (2014)
DOI: 10.1159/000356656

36. Y. M. Wei, X. Li, M. Xu, J. M. Abais, Y. Chen, C. R. Riebling, K. M. Boini, P. L. Li and Y. Zhang: Enhancement of autophagy by simvastatin through inhibition of Rac1-mTOR signaling pathway in coronary arterial myocytes. Cell Physiol Biochem, 31(6), 925-37 (2013)
DOI: 10.1159/000350111

37. S. Guixe-Muntet, F. C. de Mesquita, S. Vila, V. Hernandez-Gea, C. Peralta, J. C. Garcia-Pagan, J. Bosch and J. Gracia-Sancho: Cross-talk between autophagy and KLF2 determines endothelial cell phenotype and microvascular function in acute liver injury. J Hepatol, 66(1), 86-94 (2017)
DOI: 10.1016/j.jhep.2016.07.051

38. X. Yuan, O. Bhat, N. Meng, H. Lohner and P. L. Li: Protective Role of Autophagy in Nlrp3 Inflammasome Activation and Medial Thickening of Mouse Coronary Arteries. Am J Pathol (2018)

© 1996-2020

DOI: 10.1016/j.ajpath.2018.08.014

39. E. Steingrimsson, N. G. Copeland and N. A. Jenkins: Melanocytes and the microphthalmia transcription factor network. Annu Rev Genet, 38, 365-411 (2004)
DOI: 10.1146/annurev.genet.38.072902.092717

40. G. Napolitano and A. Ballabio: TFEB at a glance. J Cell Sci, 129(13), 2475-81 (2016)
DOI: 10.1242/jcs.146365

41. M. Palmieri, S. Impey, H. Kang, A. di Ronza, C. Pelz, M. Sardiello and A. Ballabio: Characterization of the CLEAR network reveals an integrated control of cellular clearance pathways. Hum Mol Genet, 20(19), 3852-66 (2011)
DOI: 10.1093/hmg/ddr306

42. H. Pi, M. Li, L. Tian, Z. Yang, Z. Yu and Z. Zhou: Enhancing lysosomal biogenesis and autophagic flux by activating the transcription factor EB protects against cadmium-induced neurotoxicity. Sci Rep, 7, 43466 (2017)
DOI: 10.1038/srep43466

43. P. C. Trivedi, J. J. Bartlett, L. J. Perez, K. R. Brunt, J. F. Legare, A. Hassan, P. C. Kienesberger and T. Pulinilkunnil: Glucolipotoxicity diminishes cardiomyocyte TFEB and inhibits lysosomal autophagy during obesity and diabetes. Biochim Biophys Acta, 1861(12 Pt A), 1893-1910 (2016)
DOI: 10.1016/j.bbalip.2016.09.004

44. J. Zhang, J. Wang, J. Xu, Y. Lu, J. Jiang, L. Wang, H. M. Shen and D. Xia: Curcumin targets the TFEB-lysosome pathway for induction of autophagy. Oncotarget, 7(46), 75659-75671 (2016)
DOI: 10.18632/oncotarget.12318

45. R. Emanuel, I. Sergin, S. Bhattacharya, J. Turner, S. Epelman, C. Settembre, A. Diwan, A. Ballabio and B. Razani: Induction of lysosomal biogenesis in atherosclerotic macrophages can rescue lipid-induced lysosomal dysfunction and downstream sequelae. Arterioscler Thromb Vasc Biol, 34(9), 1942-1952 (2014)
DOI: 10.1161/ATVBAHA.114.303342

46. H. Lu, Y. Fan, C. Qiao, W. Liang, W. Hu, T. Zhu, J. Zhang and Y. E. Chen: TFEB inhibits endothelial cell inflammation and reduces atherosclerosis. Sci Signal, 10(464) (2017)
DOI: 10.1126/scisignal.aah4214

Abbreviations: ECIS: electrical cell-substrate impedance sensing (ECIS); HMGB1: high mobility group box protein-1; MVEC: mouse microvascular endothelial cells; Nlrp3: NOD-like receptor family pyrin domain containing 3; ROS: reactive oxygen species; TEER: transendothelial electrical resistance; TFEB: transcription factor EB

Key Words: Free Fatty Acid, Inflammasome, Statin, Lysosome, Autophagy, Endothelial Hyperpermeability

Send correspondence to: Xiang Li, Department of Pharmacological & Pharmaceutical Sciences, College of Pharmacy, University of Houston, Houston, TX 77204-5056, Tel: 7137437978, Fax: 7137431259, E-mail: 33TUxli61@central.uh.eduU33T

© 1996-2020